

Tunneling conductance of a two-dimensional electron gas with Rashba spin-orbit coupling

B. Srisongmuang and P. Pairor*

*School of Physics, Institute of Science,
Suranaree University of Technology, Thailand*

M. Berciu

*Department of Physics and Astronomy,
University of British Columbia, British Columbia, Canada*

(Dated: May 28, 2008)

Abstract

We theoretically studied the in-plane tunneling spectroscopy of the hybrid structure composed of a metal and two-dimensional electron gas with Rashba spin-orbit coupling. We found that the energy spacing between two distinct features in the conductance spectrum can be used to measure the Rashba energy. We also considered the effect that varying the probability of spin-conserving and spin-flip scattering at the interface has on the overall conductance. Surprisingly, an increase in interface scattering probability can actually result in increased conductance under certain conditions. Particularly, in the tunneling regime, an increase in spin-flip scattering probability enhances the conductance. It is also found that the interfacial scattering greatly affects the spin polarization of the conductance in metal, but hardly affects that in the Rashba system.

PACS numbers: 73.40.Ns, 73.40.Gk, 73.23.-b, 72.25.Dc, 72.25.Mk

*Electronic address: pairor@sut.ac.th

I. INTRODUCTION

Structural inversion asymmetry of the confining electrostatic potential results in an intrinsic spin-orbit coupling of electrons in a two-dimensional (2D) electron gas (EG), which can be described by the Rashba Hamiltonian [1, 2, 3]:

$$\mathcal{H} = \frac{\vec{p}^2}{2m^*} - \lambda \hat{j} \cdot (\vec{p} \times \vec{\sigma}) \quad (1)$$

where \vec{p} is 2D momentum, m^* is the electron effective mass, \hat{j} is the direction perpendicular to the plane of motion, λ is the spin-orbit coupling parameter, which can be tuned by applying an external gate voltage perpendicular to the 2D plane, and the components of $\vec{\sigma}$ are the Pauli spin matrices. The spin-orbit interaction lifts the spin degeneracy and causes the original parabolic energy spectrum to split into two branches: $E_{\vec{k},\pm} = \frac{\hbar^2 k^2}{2m^*} \pm \hbar \lambda k$, where k is the magnitude of the wave vector. The density of states of this system is the same as that of the 2D free electron gas for all energies higher than the crossing point of the two branches. However, at the bottom of the band, the density of states has $E^{-\frac{1}{2}}$ van Hove singularity because the minus branch has an annular minimum for $k = k_0 \equiv m^* \lambda / \hbar$ instead of a single-point minimum as in the free electron gas. These properties lead to interesting phenomena, like the spin hall effect (see e.g. Refs. [4] for review), and to applications in spintronics (see e.g. Refs. [5] for review).

The Rashba effect has been seen in many systems like surface alloys and semiconductor heterostructures. Several techniques have been used to study the spin-split states in these systems. For instance, angle-resolved photoemission spectroscopy [6, 7, 8, 9, 10] and scanning tunneling microscopy [11] are used in surface alloys. The former technique is utilized mainly to obtain the energy dispersion and the Fermi surface map, from which the effective mass, the magnitude of the band splitting, and hence the Rashba spin-orbit coupling energy, $E_\lambda \equiv \hbar^2 k_0^2 / (2m^*)$, can be extracted [6, 7, 8, 9, 10]. In the latter technique, the electric current is driven through a sharp tip perpendicular to the 2D plane and the differential conductance (dI/dV) spectrum can be obtained. One can deduce the Rashba energy by fitting the dI/dV spectrum to the local density of states of the 2DEG [11]. In both cases, to obtain information about the Rashba spin-orbit coupling, extensive data fitting is needed.

In semiconductor heterostructures, the Rashba energy is measured using the Shubnikov-de Haas oscillations [12, 13]. The existence of the spin splitting at the Fermi energy leads to beating in the oscillations and the Rashba energy can be deduced from the position of the

beating node. However, because this technique is done in the presence of magnetic field, it tends to provide an overestimate of the Rashba energy because it includes the effect of the Zeeman spin splitting [14].

In this article, we propose a way to measure the spin-splitting energy more directly from the experimental data: the in-plane tunneling spectroscopy. In this technique, the Rashba energy can be determined by the energy difference between two features in the conductance spectrum. The required condition for the measurement is that the energy resolution of the tunneling spectra is at least of the order of the Rashba energy itself. This condition can be easily achieved in modern tunneling measurements [15].

An intriguing property of 2DEG with Rashba spin-orbit interaction is spin-dependent transport. Many theoretical investigations have shown that both electric and spin transport in hybrid structures between the Rashba system and various materials, like metals [16, 17, 18], ferromagnets [18, 19, 20, 21], and superconductors [22], are affected by the strength of the spin-orbit coupling [16, 17, 18, 19, 20, 21, 22], the inequality of the effective masses [16, 17, 20, 21], and the transparency of the interface [19, 20, 22]. However, in these previous studies, only spin-conserving interfacial scattering was considered. In the presence of interfacial spin-flip scattering, the equations describing the spin-up and spin-down spin states are coupled and one expects interesting consequences of this. For instance, in the study of the tunneling conductance spectrum of a semiconductor/superconductor junction [23], the non-spin-flip scattering, when present alone, is found to suppress the Andreev reflection process and hence the subgap conductance as expected. However, when the spin-flip potential scattering is also present at the interface, their combined effect surprisingly enhances the subgap conductance [23].

Here, we consider how the scattering potential barrier affects both the conductance spectrum and the spin polarization of the conductance of a junction consisting of a metal and a Rashba system. As in previous work by Zutic and Das Sarma [23], we find that the conductance spectrum, which is usually suppressed in the presence of the interfacial scattering, can be enhanced by the combined effect of both types of scattering. We also find that the spin polarizations of conductance of the metal and the Rashba system are not equal. The spin polarization in the latter depends weakly on interfacial scattering, while that in the former is greatly affected. This suggests that a spin imbalance in the Rashba system is robust against variation in the quality of the junction interface.

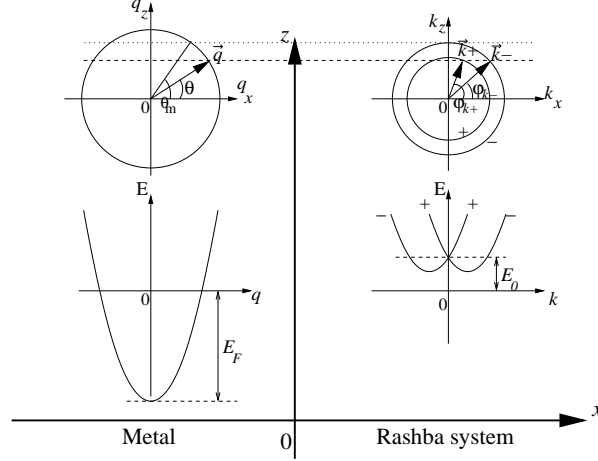


FIG. 1: The top sketches are the energy contours of the electron in the metal (left) and the Rashba system (right). The angles θ and φ are defined as those between the x axis and the momenta of electrons in the metal and the Rashba system respectively. The dashed line that crosses both sides shows the momentum states with the same k_z . The dotted line is the line of the maximum value of k_z , which defines the maximum incident angle θ_m . The lower sketches are the corresponding energy spectra (E vs the magnitude of momentum). E_F and E_0 are the metal Fermi energy and the off-set energy of the Rashba system respectively.

In the next section, we describe the theoretical method and assumptions. In Section III, we provide the results and discussion. The conclusion is given in the last section.

II. METHOD OF CALCULATION AND ASSUMPTIONS

We represent our junction by an infinite 2D system which lies on xz plane, where the metal and the Rashba system occupy the $x < 0$ and $x > 0$ region respectively. The two regions are separated by a flat interface at $x = 0$. The interfacial scattering is modeled by a Dirac delta function potential [24]. We consider ballistic transport in our junction. In the one-band effective-mass approximation, we describe our system by the following Hamiltonian:

$$\mathcal{H} = \left(\hat{p} \frac{1}{2m(x)} \hat{p} + V(x, z) \right) \mathcal{I} + \mathcal{H}_R(x). \quad (2)$$

Each term is the 2×2 matrix acting on spinor states. $\hat{p} = -i\hbar \left(\hat{x} \frac{\partial}{\partial x} + \hat{z} \frac{\partial}{\partial z} \right)$. The effective mass $m(x)$ is position-dependent, i. e., $[m(x)]^{-1} = m^{-1}\Theta(-x) + (m^*)^{-1}\Theta(x)$, where m and

m^* are effective electron masses in the metal and the Rashba system respectively, and $\Theta(x)$ is the Heaviside step function. $V(x, z)$ is also a position-dependent function and is modeled by the expression

$$V(x, z) = H\delta(x) + E_0\Theta(x) - E_F\Theta(-x) \quad (3)$$

where H represents the scattering potential at the interface, E_0 is the energy difference between the Fermi level and the bottom of the plus branch (see FIG. 1), and $E_F = \hbar^2 q_F^2 / (2m)$ is the Fermi energy of the metal. We assume that E_F is much larger than E_0 . The diagonal elements of H , $H_{\uparrow\uparrow}$ and $H_{\downarrow\downarrow}$ correspond to the non-spin-flip scattering potential characterizing the quality of the junction, while $H_{\uparrow\downarrow} = H_{\downarrow\uparrow}$ describe spin-flip scattering [23]. The Rashba Hamiltonian is written as [25]

$$\mathcal{H}_R(x) = \frac{\hat{j}}{2} \cdot [\lambda(x) (\vec{p} \times \vec{\sigma}) + (\vec{p} \times \vec{\sigma}) \lambda(x)] \quad (4)$$

where $\lambda(x) = \lambda\Theta(x)$.

From the Hamiltonian, one can obtain the eigenstates and eigenenergy for the electrons in each region as follows. In the $x < 0$ region, the energy spectrum is

$$E(q) = \frac{\hbar^2 q^2}{2m} - E_F \quad (5)$$

where $q = \sqrt{q_x^2 + q_z^2}$ is the magnitude of the 2D momentum of the electrons. In the $x > 0$ region, the eigenenergy is obtained as

$$E^\pm(k) = \frac{\hbar^2 k^2}{2m^*} \pm \frac{\hbar^2 k_0^2}{2m^*} + E_0 \quad (6)$$

where $k = \sqrt{k_x^2 + k_z^2}$ is the magnitude of the 2D momentum and $k_0 = m^* \lambda / \hbar$. FIG. 1 shows the energy spectra and energy contours of the excitations in both sides of the junction.

The wave function of the electrons in metal is written as a linear combination of incoming momentum state with equal spin components and a reflected state of the same energy and k_z :

$$\Psi_M(x, z) = \left(\frac{1}{\sqrt{2}} \begin{bmatrix} 1 \\ 1 \end{bmatrix} e^{iq_x x} + \begin{bmatrix} b_\uparrow \\ b_\downarrow \end{bmatrix} e^{-iq_x x} \right) e^{ik_z z} \quad (7)$$

where the b_\uparrow, b_\downarrow are the amplitudes for reflection of spin-up and spin-down electrons respectively. $q_x = q \cos \theta$ and $k_z = q \sin \theta$, where θ is the angle between \vec{q} and the x axis. The magnitude of the momentum, q , depends on energy as

$$q = \sqrt{\frac{2m}{\hbar^2} (-E + E_F)} \quad (8)$$

Similarly, in the Rashba system, the wave function is obtained as a linear combination of two outgoing eigenstates of the same energy and k_z :

$$\Psi_{RS}(x, z) = \left(c_+ \begin{bmatrix} \cos \frac{\varphi_{k^+}}{2} \\ \pm \sin \frac{\varphi_{k^+}}{2} \end{bmatrix} e^{\mp i k_x^+ x} + c_- \begin{bmatrix} \sin \frac{\varphi_{k^-}}{2} \\ \cos \frac{\varphi_{k^-}}{2} \end{bmatrix} e^{i k_x^- x} \right) e^{i k_z z} \quad (9)$$

where φ_{k^\pm} are the angles between \vec{k}^\pm and the x axis. For $E > E_0$, c_+ and c_- are the transmission amplitudes of electrons to plus and minus branch respectively. When $E < E_0$, c_+ and c_- refer to the transmission amplitudes of electrons to states with smaller and larger k of the minus branch respectively. The upper and lower signs in the first term of Eq. (9) are for $E \leq E_0$ and $E > E_0$ respectively. $k_x^\pm = k^\pm \cos \varphi_{k^\pm}$ and $k_z = k^\pm \sin \varphi_{k^\pm}$, where the magnitudes of the momenta, k^\pm , depend on energy as

$$k^- = k_0 + \sqrt{k_0^2 + \frac{2m^*}{\hbar^2}(E - E_0)} \quad (10)$$

$$k^+ = \pm \left(k_0 - \sqrt{k_0^2 + \frac{2m^*}{\hbar^2}(E - E_0)} \right) \quad (11)$$

Again, in Eq. (11) the upper and lower signs are for $E \leq E_0$ and $E > E_0$ respectively. The relationship between the angles φ_{k^\pm} and θ is

$$k^\pm \sin \varphi_{k^\pm} = q \sin \theta. \quad (12)$$

We can obtain the probability amplitudes $b_\uparrow, b_\downarrow, c_+$ and c_- from the following matching conditions that ensure probability conservation [25].

$$\Psi_M(x=0, z) = \Psi_{RS}(x=0, z) \equiv \Psi_0, \quad (13)$$

$$\frac{m}{m^*} \frac{\partial \Psi_{RS}}{\partial x} \Big|_{x=0} - \frac{\partial \Psi_M}{\partial x} \Big|_{x=0} = \left(2q_F \mathcal{Z} - i \frac{m}{m^*} k_0 \sigma_z \right) \Psi_0, \quad (14)$$

where $\mathcal{Z} = mH/(\hbar^2 q_F)$. The diagonal elements of \mathcal{Z} will henceforth be referred to as $Z_u \equiv Z_{\uparrow\uparrow}$ and $Z_d \equiv Z_{\downarrow\downarrow}$, while the off-diagonal element will be denoted by $Z_F = Z_{\uparrow\downarrow} = Z_{\downarrow\uparrow}$. In what follows the spin flip term Z_F will be responsible for the enhancement of a feature at the branch-crossing point in the conductance spectrum.

The particle current density along the x direction is obtained from

$$j_x^p = \frac{1}{2} \left[\Psi^\dagger(x) \hat{v}_x \Psi(x) + (\hat{v}_x \Psi(x))^\dagger \Psi(x) \right], \quad (15)$$

where $\Psi(x)$ is the spinor wave function, and $\hat{v}_x = d\hat{x}/dt = i[\mathcal{H}(x), \hat{x}]/\hbar$. From the current density, the reflection and transmission probabilities can be obtained:

$$R_{\uparrow} = |b_{\uparrow}|^2 \quad (16)$$

$$R_{\downarrow} = |b_{\downarrow}|^2 \quad (17)$$

$$T_{+} = \frac{m}{m^*} |c_{+}|^2 \left(\frac{\mp k_x^{+} + k_0 \cos \varphi_{k_x^{+}}}{q_x} \right) \quad (18)$$

$$T_{-} = \frac{m}{m^*} |c_{-}|^2 \left(\frac{k_x^{-} - k_0 \cos \varphi_{k_x^{-}}}{q_x} \right) \quad (19)$$

where $R_{\uparrow}, R_{\downarrow}$ are the reflection probabilities to spin-up and spin-down states, and T_{+}, T_{-} are the corresponding transmission probabilities. Also, the upper and lower signs in T_{+} are for $E \leq E_0$ and $E > E_0$ respectively. As mentioned earlier, the matching conditions ensure that $R_{\uparrow} + R_{\downarrow} + T_{+} + T_{-} = 1$.

Since the current is independent of x , we consider the current density in the metal for simplicity. It can be written as a function of applied voltage V as follows.

$$j_x^e(eV) = \sum_{q_x > 0, q_z} ev_x (1 - R_{\uparrow} - R_{\downarrow}) [f(E_q - eV) - f(E_q)] \quad (20)$$

where e is the electron charge, v_x is the x component of the electron group velocity, and $f(E)$ is Fermi distribution function.

By changing the integration variable and setting temperature to zero for simplicity, one can obtain the expression for the electric current as

$$j_x^e(eV) = \frac{e}{h} \frac{\mathcal{L}^2 q_F}{2\pi} \int_0^{eV} dE \int_{-\theta_m}^{\theta_m} d\theta \cos \theta \sqrt{1 - \frac{E}{E_F}} (1 - R_{\uparrow} - R_{\downarrow}) \quad (21)$$

where \mathcal{L}^2 is the area of the metal and θ_m is the maximum angle of the incident electrons from the metal (see FIG. 1): $\theta_m = \sin^{-1}(k^{-}(E)/q(E))$. Thus, the differential conductance $G(V) \equiv dj_x^e/dV$ at zero temperature is

$$G(V) = \frac{e^2}{h} \frac{\mathcal{L}^2 q_F}{2\pi} \int_{-\theta_m}^{\theta_m} d\theta \cos \theta \sqrt{1 - \frac{eV}{E_F}} (1 - R_{\uparrow} - R_{\downarrow}) \quad (22)$$

The finite temperature will smear the features in the conductance spectrum but will not change their positions (assuming that the strength of the Rashba spin-orbit coupling does not depend on temperature).

The spin polarization of the conductance \mathcal{P} is defined as

$$\mathcal{P}(E) = \frac{\sum_{q_x > 0, q_z} (n_{\uparrow} v_{\uparrow} - n_{\downarrow} v_{\downarrow})}{\sum_{q_x > 0, q_z} (n_{\uparrow} v_{\uparrow} + n_{\downarrow} v_{\downarrow})}, \quad (23)$$

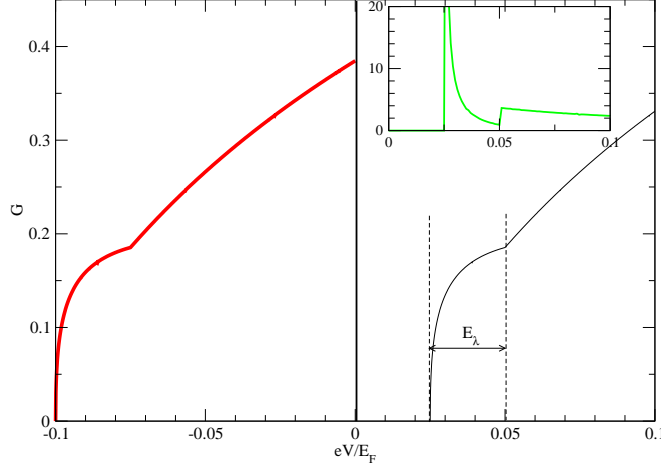


FIG. 2: On the left side is the spectrum in the case where the energy band of the Rashba system is occupied ($E_0 = -0.075E_F$) and on the right is that where the band is unoccupied ($E_0 = 0.05E_F$). Z and Z_F are set equal to zero. $m/m^* = 10$ and $k_0 = 0.05q_F$. The derivative of the conductance spectrum on the right (dG/dV) is shown in the inset.

where $n_\sigma v_\sigma$ is the number of electrons with spin σ that cross a plane of interest per unit time. In terms of the reflection probabilities this spin polarization in the metal can be written as

$$\mathcal{P}_M(E) = \frac{\sum_{q_x > 0, q_z} (-R_\uparrow + R_\downarrow)}{\sum_{q_x > 0, q_z} (1 - R_\uparrow - R_\downarrow)} \quad (24)$$

and the spin polarization in the Rashba system in terms of the transmission probabilities is written as

$$\mathcal{P}_{RS}(E) = \frac{\sum_{q_x > 0, q_z} (T_+ \cos \varphi_{k^+} - T_- \cos \varphi_{k^-})}{\sum_{q_x > 0, q_z} (T_+ + T_-)} \quad (25)$$

As expected, the spin polarization measures the difference in number of the carriers with spin-up and spin-down on each side.

III. RESULTS AND DISCUSSION

In this section, we discuss the effect of the interfacial scattering on the differential conductance spectra and the spin polarization of conductance on each side of the junction. In all plots, we set $m/m^* = 10$ and $k_0 = 0.05q_F$, which corresponds to typical experimental values in metal/Rashba system junctions [23, 26]. In FIG. 2, two conductance plots for two values of E_0 are shown. Positives values of E_0 means the energy spectrum of the Rashba

system is unoccupied and the positive eV across the junction will cause the current to flow from the metal to the Rashba system.

In the case shown in FIG. II where the energy spectrum is occupied ($E_0 = -0.075E_F$), the results are identical in shape to those in the unoccupied case ($E_0 = +0.05E_F$), but the applied voltage eV across the junction has to be negative. There are two main features at the voltage corresponding to the bottom and the branch-crossing of the energy band. The distance between them depends on E_λ , which is the quantity of interest. The value of E_0 is not important, i. e., changing E_0 causes a rigid shift in energy, and will henceforth be set equal to zero.

We do not consider the spin filtering interface. That is, we set the non-spin-flip scattering strength $Z_u = Z_d = Z$. It is well-known that the difference in Z_u and Z_d will cause a spin-filtering effect. That is, a higher Z_u will make the transport of the spin-up electrons less favorable and vice versa. This effect cannot be seen in the conductance spectrum and will not be considered in the spin polarization.

A. Differential conductance spectra

In all conductance plots, the conductance is in units of $e^2\mathcal{L}^2q_F/(2\pi h)$. The conductance spectra G with different Z_F in different limits of Z are shown in FIG. 3. Junctions with metallic contacts are characterized by $Z \ll 1$, whereas those in the tunneling limit are characterized by $Z \geq 1$. In general, the conductance is zero until the applied voltage reaches $eV = -E_\lambda$, which is the bottom of the band of the Rashba system. The conductance increases suddenly with large initial slope that decreases steadily until a second feature: the kink occurring at $eV = 0$, which is the crossing point of the two branches of the band. After this point, the conductance increases approximately linearly. In the presence of Z_F , there occurs a discontinuity in the conductance at $eV = 0$. The height of the jump depends on both Z and Z_F . The energy difference between the onset and the discontinuity in slope of the conductance spectrum can be used to measure the magnitude of the Rashba energy E_λ .

In addition to the influence on the discontinuity at $eV = 0$, the interfacial scattering affects the overall conductance spectrum as well. For metallic contacts, the spin-flip scattering suppresses the conductance as expected. However, in the intermediate and the tunneling limits, the results are rather surprising. As can be seen in FIG. 3(b) when $Z = 0.5$, the

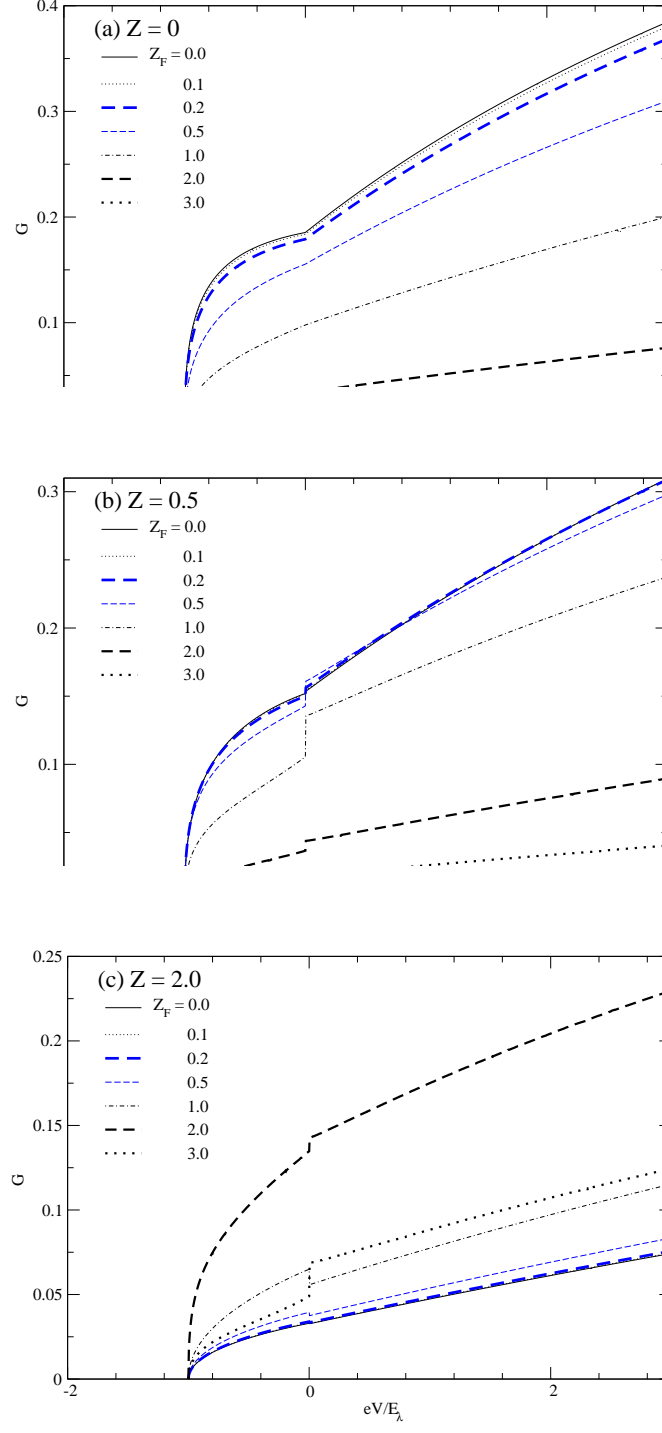


FIG. 3: Differential conductance spectra G for different Z_F in the case where (a) $Z = 0$, (b) $Z = 0.5$, and (c) $Z = 2.0$.

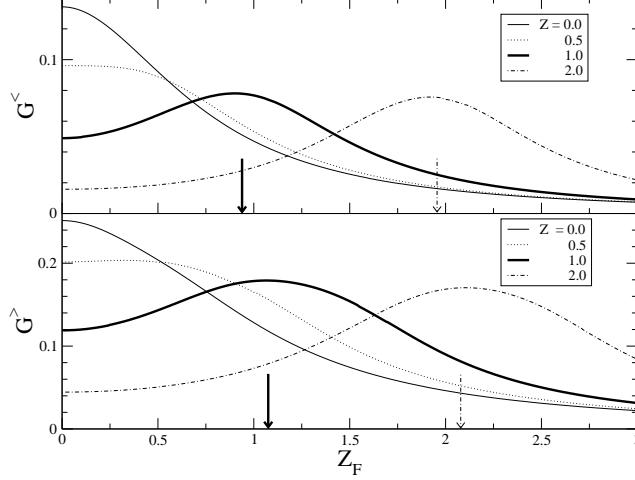


FIG. 4: Differential conductance $G(eV)$ plotted as a function of the spin-flip barrier height Z_F at a constant energy eV slightly below [upper panel, denoted by $G^<(Z_F)$] and slightly above [lower panel, denoted by $G^>(Z_F)$] the energy corresponding to the crossing of the Rashba-split bands. The arrows indicate the values of Z_F^* , where the maximum differential conductances $G^>$ and $G^<$ occur, for $Z = 1.0$ (thick arrows) and 2.0 (dashed-dotted arrows).

increase in Z_F from zero to a small value (less than 0.5) does not affect the conductance much. Only when Z_F is increased beyond 0.5, does the conductance get suppressed. When Z is high, e. g. $Z = 2.0$ as in FIG. 3(c), the conductance spectrum can be enhanced by the increase in Z_F up to a value Z_F^* , after which the spectrum becomes suppressed. Z_F^* is found to depend strongly on Z .

One can see the effect on the conductance spectrum of spin-flip scattering more clearly by considering plots of the conductance G as a function of Z_F for energies just below and just above 0. In FIG. 4, $G^< \equiv G(-\delta)$ and $G^> \equiv G(+\delta)$, where $\delta/E_\lambda = 0.8$, are plotted as a function of Z_F for different values of Z . For small Z , both $G^>$ and $G^<$ decrease with Z_F as expected. However, this trend starts to change when Z is higher than 0.5. That is, both $G^>$ and $G^<$ increase with Z_F and reach a maximum value at Z_F^* (as indicated by arrows in FIG. 4), after which they decrease with Z_F . Notice that Z_F^* is a little smaller for $G^<$ than for $G^>$ and is approximately equal to Z . It should be noted that a similar dependence of both $G^>$ and $G^<$ on Z can also be seen, if one plots $G^>$ and $G^<$ as a function of Z instead.

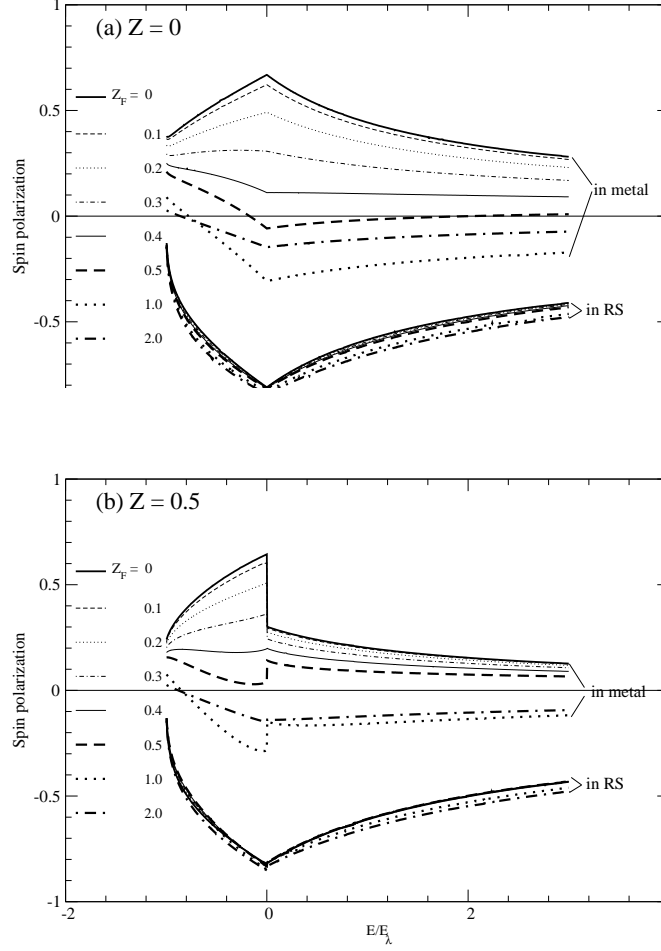


FIG. 5: The plots of the spin polarization of conductance in metal and Rashba system (RS) as a function of energy when Z is (a) 0 and (b) 0.5.

B. Spin polarization of conductance

The plots of the spin polarizations in both metal and Rashba system as a function of energy are shown in FIG. 5. The spin polarizations of the two sides are very different. In Rashba system, it is always negative, whereas in the metal it is positive when the spin-flip scattering is not strong. This may be understood by considering the density of states of the Rashba system.

The density of states of the minus branch is larger than that of the plus branch. As we can see from FIG. 6, because the spins of the transmitted states of the minus branch are mostly pointing down, it is not surprising that the spin polarization in the Rashba system is negative. As for the metal side, because more spin-down states are transmitted into the

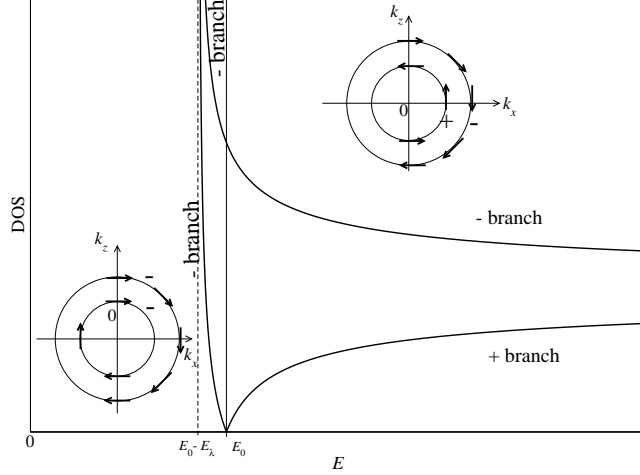


FIG. 6: Density of states of each branch of the 2DEG with the Rashba spin-orbit coupling. The contour plots on the left and on the right are those in the case where $E < E_0$ and $E > E_0$ respectively. When $E > E_0$, the outer contour is that of - branch and the inner one is that of + branch. When $E < E_0$, both energy contours belong to the - branch. The arrows represent the spin direction of the states with positive v_x .

Rashba system, the spin polarization is positive.

The interfacial scattering does not affect the spin polarization in the Rashba system as much as in the metal. The increase in either Z or Z_F seems to slightly change the magnitude of the spin polarization. However, in metal the interfacial scattering potential affects the spin polarization a great deal. For a particular value of Z , the increase in Z_F can cause the spin polarization in metal to change sign.

IV. CONCLUSIONS

According to the results from our simple model, one can directly use in-plane tunneling conductance spectrum to measure the Rashba energy of a system with the Rashba spin-orbit coupling. The energy difference between the onset and the discontinuity in slope of the conductance spectrum is equal to the Rashba energy. Both features are found to be robust against variation in the quality of the junction.

Experimentally, to be able to measure the Rashba energy, the required energy resolution is at least of the order of the Rashba energy itself and the temperature is low enough in order

that both features are visible. The Rashba energies in semiconductor-based heterostructures such as InAs, InGaAs and GaN, are of order 1 meV [27, 28, 29, 30, 31, 32], whereas those of surface alloys like Li/W(110), Pb/Ag(111), and Bi/Ag(111) can be as large as 200 meV [11, 33, 34, 35]. These conditions can be readily met in modern tunneling measurements [15].

We also found that as the current is driven through the system, an imbalance of spin in both sides occurs. The spin polarization of the conductance in the metal is found to depend strongly on both types of the interfacial scattering and can disappear when the barrier is in the tunneling regimes. On the contrary, in the Rashba system the spin polarization is always present and only slightly affected by interfacial scattering. This finding suggests that the spin imbalance caused by current flow in the system with the Rashba spin-orbit coupling is robust against variation in the quality of the junction as well.

Acknowledgments

We thank Dr. Michael F. Smith for critical reading of the manuscript. Also, we would like to acknowledge financial support from Cooperative Research Network (Physics). P.P. thanks Thai Research Fund and Commission on Higher Education, Thailand (grant no. RMU488012 and CHE-RES-RG "Theoretical Physics") for financial support. M.B. was supported by the Research Corporation, CIFAR and NSERC.

-
- [1] E. I. Rashba, Sov. Phys. Solid State **2**, 1109 (1960).
 - [2] Y. A. Bychkov and E. I. Rashba, J. Phys. C **17**, 6039 (1984).
 - [3] Y. A. Bychkov and E. I. Rashba, JETP Lett. **39**, 78 (1984).
 - [4] H. Engel, E. I. Rashba, and B. I. Halperin, *Handbook of Magnetism and Advanced Magnetic Materials* (Chichester: John Wiley and Sons Limited, 2007).
 - [5] I. Zutic, J. Fabian, and S. Das Sarma, Rev. Mod. Phys. **76**, 323 (2004).
 - [6] S. LaShell, B. A. McDougall, and E. Jensen, Phys. Rev. Lett. **77**, 3419 (1996).
 - [7] F. Reinert, J. Phys.: Condens. Matter **15**, S693 (2003).
 - [8] J. Henk, M. Hoesch, J. Osterwalder, A. Ernst, and P. Bruno, J. Phys.: Condens. Matter **16**, 7581 (2004).

- [9] H. Cercellier, Y. Fagot-Revurat, B. Kierren, F. Reinert, D. Popović, D. and Malterre, Phys. Rev. B **70**, 193412 (2004).
- [10] D. Popović, F. Reinert, S. Hufner, V. G. Grigoryan, M. Springborg, H. Cercellier, Y. Fagot-Revurat, B. Kierren, and D. Malterre, Phys. Rev. B **72**, 045419 (2005).
- [11] C. R. Ast, G. Wittich, P. Wahl, R. Vogelgesang, D. Pacilé, M. C. Falub, L. Moreschini, M. Papagno, M. Grioni, and K. Kern, Phys. Rev. B **75**, R201401 (2007).
- [12] J. Nitta, T. Akazaki, H. Takayanagi, and T. Enoki, Phys. Rev. Lett. **78**, 1335 (1997).
- [13] G. Engels, J. Lange, Th. Schäpers, H. and Lüth H, Phys. Rev. B **55**, R1958 (1997).
- [14] G. Lommer, F. Malcher, and U. Rössler, Phys. Rev. Lett. **60**, 728 (1988).
- [15] E. L. Wolf, *Principles of tunneling spectroscopy* (Oxford University Press, New York, 1989).
- [16] G. Liu and G. Zhou, Chin. Phys. Lett. **22**, 3159 (2005).
- [17] M. Lee and M. Choi, Phys. Rev. B **71**, 153306 (2005).
- [18] V. M. Ramaglia, D. Bercioux, V. Cataudella, G. De Filippis, C. A. Perroni, and F. Ventriglia, Eur. Phys. J. B **19**, 365 (2003).
- [19] C. M. Hu and T. Matsuyama, Phys. Rev. Lett. **87**, 066803 (2001).
- [20] T. Matsuyama, C. M. Hu, M. Grundler, G. Meier, and U. Merkt, Phys. Rev. B **65**, 153322 (2005).
- [21] Y. Jiang and M. B. A. Jalil, J. Phys.: Condens. Matter **15**, L31 (2003).
- [22] T. Yokoyama, Y. Tanaka, and J. Inoue, Phys. Rev. B **74**, 035318 (2006).
- [23] I. Zutic and S. Das Sarma, Phys. Rev. B **60**, R16322 (1999).
- [24] G. E. Blonder, M. Tinkham, and T. M. Klapwijk, Phys. Rev. B **25**, 4515 (1982).
- [25] U. Zülicke and C. Schroll, Phys. Rev. Lett. **88**, 029701 (2002).
- [26] T. Koga, J. Nitta, H. Taganayagi, and S. Datta, Phys. Rev. Lett. **88**, 126601 (2002).
- [27] S. Sasa, K. Anjiki, T. Yamaguchi, and M. Inoue, Physica B **272**, 149 (1999).
- [28] D. Grundler, Phys. Rev. Lett. **26**, 6074 (2000).
- [29] T. Matsuyama, R. Kürsten, C. Meibner, and U. Merk, Phys. Rev. B **61**, 15588 (2000).
- [30] T. Koga, J. Nitta, T. Akazaki, and H. Takayanagi, Phys. Rev. Lett. **89**, 046801 (2002).
- [31] K. Fujii, Y. Morikami, T. Ohyama, S. Gozu, and S. Yamada, Physica E **12**, 434 (2002).
- [32] L. Ikai, J. K. Tsai, W. J. Yao, P. C. Ho, L. W. Tu, T. C. Chang, S. Elhamri, W. C. Mitchel, K. Y. Hsieh, J. H. Huang, H. L. Huang, and W. C. Tsai, Phys. Rev. B **65**, 161306 (2002).
- [33] E. Rotenberg, J. W. Chung, and S. D. Kevan, Phys. Rev. Lett. **82**, 4066 (1999).

- [34] D. Pacilé, C. R. Ast, M. Papagno, C. Da Silva, L. Moreschini, M. Falub, A. P. Seitsonen, and M. Grioni, Phys. Rev. B **73**, 245429 (2006).
- [35] C. R. Ast, J. Henk, A. Ernst, L. Moreschini, M. C. Falub, D. Pacilé, P. Bruno, K. Kern, and M. Grioni, Phys. Rev. Lett. **98**, 186807 (2007).